Conceptual design study to determine optimal enclosure vent configuration for the Maunakea Spectroscopic Explorer (MSE)

Kei Szeto, Konstantinos Vogiatzis, Horia Hangan, Chowdhury M. Jubayer, Craig Breckenridge, et al.

Kei Szeto, Konstantinos Vogiatzis, Horia Hangan, Chowdhury M. Jubayer, Craig Breckenridge, Nathan Loewen, Steven Bauman, Derrick Salmon, "Conceptual design study to determine optimal enclosure vent configuration for the Maunakea Spectroscopic Explorer (MSE)," Proc. SPIE 9145, Ground-based and Airborne Telescopes V, 91450A (22 July 2014); doi: 10.1117/12.2056728

Event: SPIE Astronomical Telescopes + Instrumentation, 2014, Montréal, Quebec, Canada

Conceptual design study to determine optimal enclosure vent configuration for the Maunakea Spectroscopic Explorer (MSE)

Kei Szeto[1a], Konstantinos Vogiatzis[b], Horia Hangan[c], Chowdhury M. Jubayer[c], Craig Breckenridge[d], Nathan Loewen[d], Steven Bauman[e], Derrick Salmon[e]

[a]National Research Council Canada, Herzberg Institute of Astrophysics, 5071 West Saanich Road, Victoria, BC, Canada, V9E 2E7
[b]TMT Observatory Corporation, Pasadena, CA 91105, USA
[c]WindEEE Research Institute, 2535 Advanced Avenue, London, Ontario, N6M 0E2 Canada
[d]Dynamic Structures Ltd, 1515 Kingsway Avenue, Port Coquitlam , BC, Canada V3C 1S2
[e]CFHT Corporation, 65-1238 Mamalahoa Hwy, Kamuela, Hawaii 96743, USA

ABSTRACT

The Maunakea Spectroscopic Explorer (MSE; formerly Next Generation Canada-France-Hawaii Telescope) is a dedicated, 10m aperture, wide-field, fiber-fed multi-object spectroscopic facility proposed as an upgrade to the existing Canada-France-Hawaii Telescope on the summit of Mauna Kea. The enclosure vent configuration design study is the last of three studies to examine the technical feasibility of the proposed MSE baseline concept. The enclosure vent configuration study compares the aero-thermal performance of three enclosure ventilation configurations based on the predicted dome thermal seeing and air flow attenuation over the enclosure aperture opening of a Calotte design derived from computational fluid dynamics simulations. In addition, functional and operation considerations such as access and servicing of the three ventilation configurations is discussed.

Keywords: MSE, spectrograph, CFD, aero-thermal, ventilation, flushing, dome seeing, wind jitter

1. INTRODUCTION

The Maunakea Spectroscopic Explorer (MSE; formerly Next Generation Canada-France-Hawaii Telescope) is a proposal to upgrade the Canada-France-Hawaii Telescope (CFHT) to a dedicated, 10m aperture, wide-field, fiber-fed multi-object spectroscopic facility by replacing the existing 3.6m telescope with a 10m segmented-mirror telescope equipped with a multi-object fiber-fed spectrograph with reconfigurable fiber inputs at prime focus. The scientific impetus for a dedicated wide-field, multi-object spectrograph on a 10m class telescope has been recognized by the international astronomical community for more than a decade[1] and MSE will realize the potential scientific value of such a facility.

The current top level MSE requirements[2] for meeting the intended science goals are summarized in Table 1 and its baseline enclosure and telescope configuration is illustrated in Figure 1.

Table 1: Top level design requirements.

Aperture	10 m (segmented)
Field of View	1.5 deg^2 (hexagonal)
Wavelength Range	370-1300 nm
Number of Fibers	3,200 (low resolution); 800 (high resolution)
Spectral Resolution	R2,000 (370-1300 nm); R20,000 (480-680 nm)

The MSE development began as a grassroots movement within the CFHT user communities in 2010. In early 2011, a Feasibility Study report of the MSE facility was released to the CFHT board of directors validating its scientific

[1] Email: kei.szeto@nrc-cnrc.gc.ca; Telephone: 250-363-0059; Fax 250-363-0045
[2] The baseline requirements are evolving as the development of science cases of MSE progresses.

Ground-based and Airborne Telescopes V, edited by Larry M. Stepp, Roberto Gilmozzi,
Helen J. Hall, Proc. of SPIE Vol. 9145, 91450A • © 2014 SPIE
CCC code: 0277-786X/14/$18 • doi: 10.1117/12.2056728

capabilities, technical feasibility and readiness. By May 2013, the MSE project office was launched in the CFHT headquarters in Waimea, Hawaii, with a goal to advance and formalize the scientific, technical and programmatic project definitions in a Construction Proposal over the next 3 years. A companion paper by Simons[2] outlines the MSE project and its development plan. Another companion paper by McConnachie[3] reports on the current status of the science case development and the corresponding requirements flow-down of the proposed facility.

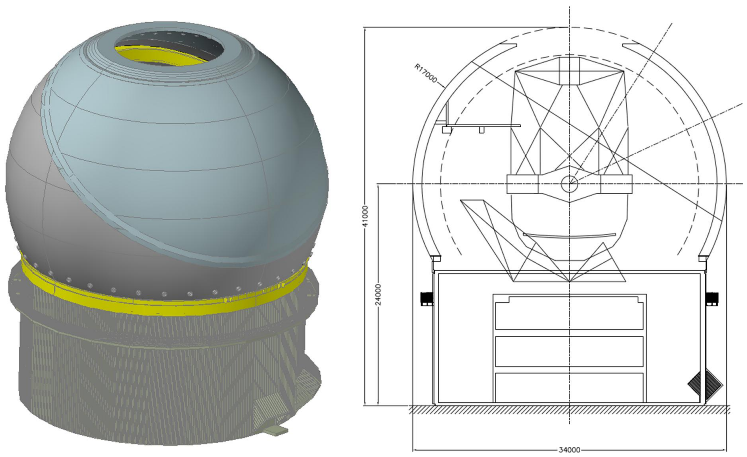

Figure 1: Baseline MSE configuration – exterior view of Calotte enclosure (left) and cross section view of the proposed enclosure and "Keck-like" telescope structure on the existing piers (right). The current enclosure concept accommodates a dome-mounted crane to service the primary mirror segments and fiber input components at the telescope top end.

In this paper, we discuss the findings of the last of three technical examinations in the Feasibility Study which was first reported in 2012 by Szeto[4]. The titles of the three technical studies conducted in succession were: 1. Telescope Pier Study – Load Capacity and Structural Interface, 2. Enclosure Fixed Base Study – Telescope and Enclosure Configuration and Load Capacity and 3. Aero-Thermal Study – Dome Thermal Seeing and Air Flow Attenuation over the Enclosure Aperture Opening.

In our previous paper, we affirmed the existing enclosure and telescope piers have sufficient capacity to support the proposed enclosure and telescope structure given minor structural reinforcement of the enclosure pier bracing. In this report, we compare the aero-thermal performance of three enclosure ventilation configurations using computational fluid dynamics (CFD) simulations to predict the thermal seeing and wind induced dynamics by the flow attenuation inside the enclosure and over its aperture opening. The optimal ventilation configuration is discussed based on performance comparison along with functional and operation considerations, such as complexity of structural and mechanical design, ease of access and servicing, and the overall facility lifetime cost.

2. VENTILATION AND CFD MODELING STRATEGIES

The proposed MSE enclosure combines characteristics from both Keck[5] and TMT[6] enclosures. Its size and aperture width are comparable to Keck but its type is the same as TMT's. Keck has successfully mitigated dome and mirror seeing by active ventilation. An exhaust fan pulls interior air through an opening on the observatory floor and discharges it through a tunnel toward the least probable wind direction away from the telescope. On the other hand, through extensive CFD aero-thermal modeling, TMT has determined three-level of vent openings on its Calotte enclosure provide sufficient passive ventilation to meeting its thermal seeing budget[7].

Therefore we decided to investigate and compare both ventilation strategies. For active ventilation, it is possible to retrofit the existing CFHT enclosure pier to accommodate a floor opening and exhaust system to vent through an existing tunnel on the west side. On the other hand, generating passive ventilation through vent openings on a Calotte enclosure is more challenging. From a mechanical design perspective, the Calotte geometry precludes placing vent doors on the upper rotating cap portion since the varying orientation of the cap makes servicing access difficult and sealing of vent openings impractical. Geometrically the remaining available "ventable" area on the rotating base is inherently asymmetric resulting in variations in ventilation efficiency as the azimuthal angle changes relative to wind direction when tracking during an observation.

Both enclosure ventilation strategies require significant mechanical investment but have intrinsically different functional considerations, as well as different construction and operating costs. In general, for the proposed MSE Calotte enclosure, passive ventilation has higher capital cost than active ventilation due the extra structure and mechanics required for the vent doors. But given reasonable mechanical reliability and maintenance requirements, passive ventilation has lower operating cost than active ventilation over the lifetime of the observatory.

2.1 Passive Ventilation - Operational and Functional Considerations

The size of the vent openings is a practical consideration. The structural concept for the enclosure consists of ribs running vertically along the longitude lines of the dome. The ribs are spaced at about 2m to support the outer dome skin. The ribs have lateral and diagonal bracing running between them. The structural system requires continuity through the region of vent openings, and the structural framing may run either between the vents or behind the vents. It follows that the vent spacing should be a multiple of the dome ribs spacing, so vent doors may be nominally 2m or 4m wide. Vent doors spanning further than 4m require significant strength to resist the exterior wind loads, and commercially available door options that meet these requirements are limited and costly.

Multiple options are available for the vent door actuation mechanisms. The main design requirements are resistance to the very high wind loads at the summit, reliability of operation, and weather sealing. Since the collective perimeter of the doors is very large, daytime air infiltration through the door seals is a major concern. From a ventilation control perspective, it is also advantageous if the amount of flow can be adjusted, either by changing the opening size or louver angle to adjust the incoming flow.

For the TMT enclosure a three-level modular door system has been proposed. The exterior doors consist of commercially available roll-up doors with high wind load ratings and the interior doors consist of insulated door panels which provide insulation and sealing against air infiltration in order to minimize thermal load on the daytime air conditioning system. The amount of flow is controlled by adjusting the height of exterior door openings while the interior doors stay fully open in operation. Moreover, an extensive access walkway system is provided at each level of the vent doors for inspection and service along with provision to replace any door components that could possibly need replacement over the life of the enclosure.

2.2 Proposed Ventilation Configurations for CFD Study

The first MSE enclosure passive ventilation configuration *#1-p* is assigned a "generous[3]" vent area with a vent design similar to TMT, 5m (H) x 4m (W), in two levels. The ideal placement of the levels is driven by two criteria. First, as much as possible, the optical path volume[4] should be flushed, i.e. "visible" by the vents, throughout the range of the telescope observing zenith angle. Second, if the enclosure surface is spherical, as is the case with the Calotte design, the vents should be confined to a zone within the dome equator. Beyond that zone air flow is no longer normal to the vent due to curvature and the vent efficiency would decrease accordingly. For ventilation configuration *#1-p*, the lower level is centered 5m below the elevation axis[5] (EA) and consists of 15 vents while the upper level is centered 1.2m above the EA and consists of 11 vents. Figure 2 (left) illustrates the first ventilation configuration *#1-p*.

An alternate ventilation configuration *#2-p*, which minimizes construction costs and maximizes mechanical simplicity, with a single level vent openings is proposed and examined. Ventilation configuration *#2-p* has only 55% of the vent area as configuration *#1-p*. The expected design, construction and servicing requirements of the 23 5m

---

[3] Maximum vent area practical on the rotation base

[4] Defined as a cylindrical volume of 10m diameter by 20m long with its base coincident on the M1 surface, see definition in Section 3.1

[5] The spherical centre of the Calotte enclosure is coincident with the centre of the telescope, i.e. the intersection point of the azimuth and elevation axes.

(H) x 2.5m (W) vent openings are comparable with the newly installed vents on CFHT[8] as shown in Figure 9. The 23 vents (at 9° interval azimuthally) are centered 3.5m below the dome equator, and directly "see" the primary mirror for zenith angles between 0° to 45°. Figure 2 (right) illustrates the second ventilation configuration *#2-p*.

The active ventilation configuration (without vent opening), *#3-a*, consists of a single opening on the west side of the observing floor, with dimensions 4m x 2.5m, centered 18.9m from the centre of the base azimuth axis. A more uniform distribution of openings around the floor might produce a better flow pattern for flushing, but it would add cost and complexity to implement in the existing enclosure pier. The nominal volume flow rate is assumed to be 90,000cfm, which is equivalent to approximately 10 air exchanges inside the dome per hour. This value is the optimum exhaust rate for Keck's ventilation[9], and, since the Keck and MSE enclosure interior volumes are comparable, this represents a natural initial choice.

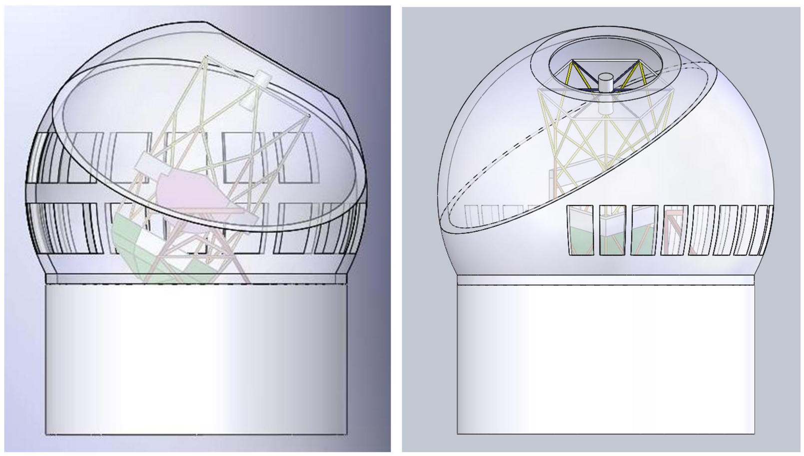

Figure 2: Ventilation configuration *#1-p* (left) – 5m x 4m vent opening, 11 vents at upper level and 15 vents at lower level; and ventilation configuration *#2-p* (right) – 5m x 2.5 m vent opening, 23 vents in a single level.

3. CFD MODELING

In this study, the geometry of the telescope, enclosure, and the summit topology are created in SolidWorks® CAD software. The mesh for the SolidWorks® model is generated using Pointwise® v17.0 and the simulations are performed using ANSYS Fluent® 13.0. Details of the CFD model properties, input parameters, boundary conditions and numerical schemes are described in this section.

3.1 Model Properties - Computational Domain, Mesh Type and Boundary Conditions

The overall dimension of the computational domain is 800m in X direction (+X is east), 500m in Y direction (+Y is North) and 300m above the origin. The height (H) of the enclosure is 41m. The upstream fetch is 11.4H, the distance to the outlet is 7.3H and the distance between the top of the enclosure and the top of the domain is 6.3H. In order to reduce the number of cells inside the computational domain and reduce computational time, practical simplifications are made to the overall geometry: for instance the truss structure, that holds the fiber input unit, is not included in the model. The mesh consists of hexahedral, prismatic and tetrahedral cells. Hexahedral cells are used at the vent openings; prismatic cells are used on the bottom of the domain with 15 layers and on the primary mirror surface with 10 layers; and tetrahedral cells are used elsewhere. The total number of cells is approximately 1.7 million. Figure 3(left) illustrates the computational domain and Figure 3(right) shows the generated mesh in the computational domain.

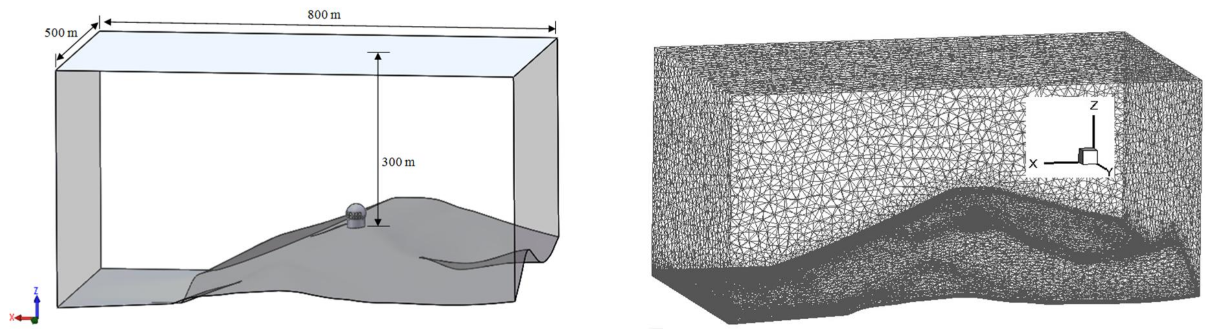

Figure 3: Computational domain (left); and Generation mesh (right).

One incoming wind direction is considered, from East to West, i.e. along the +X-axis. The East side of the domain is treated as velocity inlet type boundary. The North and South sides (+Y, -Y) and top of the domain (+Z) are treated as symmetry type boundaries. The West side of the domain (-X) is modeled as outflow type boundary. The horizontal flat part of the bottom of the domain is modeled as symmetry and the actual summit topology part of the bottom is modeled as wall.

Where possible, common CFD models are used in multiple simulations to minimize modeling effort. For example, the same model was used to study ventilation configuration *#1-p* and *#3-a*. For the passive ventilation simulation, the 26 open vents are treated as interior volumes and floor opening surface is treated as wall; for the active ventilation simulation, the outside surface of the vents are treated as walls and the floor opening is modeled as velocity outlet boundary type, i.e. velocity inlet type boundary with negative flow direction. Similarly, the same technique was used to model open and closed vents within a common model for the passive ventilation configuration *#2-p* simulations.

3.2 Input Parameters – Wind Velocities, Thermal Boundary Conditions and Air Properties

In all simulated cases the wind direction is from the East, which is the most probable for the CFHT site[10] and the telescope zenith angle is 30°. We assumed the MSE science targets follow the same statistics as for the Keck observation with the most probable zenith angles between 20° to 40°.

The range of most probable wind speeds for the CFHT site are 4m/s to 6m/s, with a median value of 7m/s. In additional, the TMT simulation results indicate the dome and mirror seeing behavior is constant for the wind velocity range from 4.5 m/s to 7m/s. Therefore a nominal value of 5m/s is selected and at this wind velocity all vents are required to be open for dome ventilation. In addition, a low wind speed value of 2m/s(10%ile), and high wind speed, closed-vent, value of 10m/s (80%ile) are selected for the passive ventilation configuration #2 p simulations.

At the domain inlet, the magnitude of the wind velocity is adjusted such that it reaches the required velocity at the CFHT location. This involves using the "speed up" factor for hill from ASCE 7-10[11]. A turbulence intensity of 5% and integral length scale of 40 m are applied at the domain inlet.

The thermal boundary conditions and the air properties used in this study are given in Table 2 and 3, respectively. The nighttime median ambient inlet temperature is 275K at the CFHT site. The corresponding exterior skin temperature of the dome is 269K, assuming white paint, and the other thermal boundary conditions listed are based on in-situ measurements and modeling results[12]. The air properties are based on a summit elevation of 4200m.

Table 2: Thermal boundary conditions

Location	Temperature (K)
Inlet	275
Exterior of the dome	269
Exterior of the fixed base	274
Ground/bottom of the domain	269
Inside dome surface and bottom of the dome	274
Mirror and M1 cell	276
Top end fiber input unit	276
All other structures	274

Table 3: Properties of air

Reference Pressure (Pa)	Reference Temperature (K)	Density (kg/m^3)	Kinematic Viscosity (m^2/s)
61000	275	0.8	2x10^{-5}

3.3 Simulation Cases - Study Conditions by Ventilation Configurations and Input Parameters

A total of seven simulation cases were simulated. The study cases and their input parameters are tabulated in Table 4. The study conditions of the seven cases were chosen incrementally as knowledge and understanding of the ventilation characteristics progresses for each ventilation configuration starting from *#1-p*. The progression of the study cases will be discussed in the summary section of this paper.

Since time and budget constraints precluded exhaustive investigation of all input parameters, the goal of this CFD study is to determine a viable ventilation configuration, active or passive, for the proposed MSE enclosure and telescope baseline configuration in context with the 2011 Feasibility Study, i.e. to identify a viable enclosure ventilation concept that minimizes design, construction and operating costs of the proposed facility.

Table 4: Details Conditions of Study Cases

Case	Ventilation Configuration	Total Number of Vents	Exhaust Flow Rate (cfm)	Azimuth Angle w.r.t. Wind Direction	Wind Speed (m/s)	Comments
1	#1-p	26	n/a	90°*	5	TMT type passive ventilation
2	#3-a	0	90,000	90°*	5	Keck type active ventilation at optimal flow rate
3	#3-a	0	180,000	90°*	5	Keck type active ventilation at 2 x optimal flow rate
4	#2-p	23	n/a	90°*	5	CFHT type passive ventilation
5	#2-p	23	n/a	180°**	5	CFHT type passive ventilation
6	#2-p	23	n/a	90°*	2	CFHT type passive ventilation
7	#2-p	0	n/a	90°*	10	Closed vents, passive ventilation through aperture opening

*South pointing
**West pointing

Three-dimensional, unsteady Reynolds Averaged Navier-Stokes (RANS) simulations are performed using the Shear Stress Transport (SST) k-ω turbulence model. The Pressure Implicit with Splitting of Operators (PISO) algorithm is used for Pressure-Velocity coupling. First order upwind schemes are used for the spatial discretization. For the transient formulation, a first order implicit scheme is used. The convergence criteria for the energy equation and Volume of Fluid (VOF) model residuals are 10^{-6} and 10^{-5}, respectively. For the rest of the equations, 10^{-4} is employed.

For Cases 1 and 2, the simulations run for a total of 480 seconds of flow time. After the first 270 seconds the VOF model is activated to monitor flushing of the air inside the telescope enclosure. However, for Cases 3-6, the simulations run for around 370s of flow time and the VOF model is activated earlier at around 160s to reduce the computational time. However, we checked and ensured that the solution is stable before activating the two phase modeling. For Case 7, the simulation run for 770s and this was the longest period of flow time used. This is because there are no vents in Case 7 and minimal passive ventilation is provided through the aperture opening.

To monitor the flushing characteristics, the air is assigned in two different phase groups. The separate phases are patched inside (phase-2) and outside (phase-1) of the enclosure. After the VOF model is activated, the time step size is manually varied to keep the Courant Number to around 1.

4. SUMMARY OF CFD SIMULATION FINDINGS

4.1 Assessment Criteria for Ventilation Performance

The major criteria for effective ventilation, passive or active, are the air volume exchange rate in the enclosure and the standard deviation of the temperature fluctuations, T_{RMS}, inside the optical volume. The Optical Volume (OV) is defined as a cylindrical volume of 10m diameter (D) and 20m in length (L) perpendicular to the primary mirror (M1) surface, and the Optical Axis (OA) is the axis of the cylinder normal to the M1 surface. The optimal enclosure design should maximize the air volume exchange rate and minimize T_{RMS}. Even though both parameters have their individual merits, ultimately it is the temperature gradients inside the enclosure that cause image quality degradation. The air exchange rate is captured by the factor Volume Fraction (VF) which is the ratio of fresh air relative to total air within the enclosure control volume (as confined by the enclosure interior skin, aperture plane, vent or floor opening planes) after a certain flow time in the simulation.

In addition, the wind speed at the telescope top end is of concern for image blur consideration. It is important to minimize telescope wind jitter by constraining the ratio of the "top end" wind speed to external wind speed to <0.2. Different ventilation configurations result in different flow patterns that alter the flow behavior near the aperture opening and at the top end. Consequently, this may result in increased wind jitter that offsets any improvements in dome seeing.

For the CFD study, three quantities are monitored for performance comparison of different ventilation configurations. They are describes below, and collectively they form the Image Quality (IQ) criterion:

- Fresh air volume fraction VF(t), spatially averaged in OV and along OA; this is a measurement of ventilation efficiency.
- Temperature $T_{MEAN}(t)$, spatially averaged in OV and along OA; T(t) should track the ambient temperature closely otherwise causes discontinuity at the aperture shear layer, where most of the dome seeing originates.
- Temperature fluctuations $T_{RMS}(t)$, spatially averaged in OV and along OA; this correlates directly to OPD_{RMS}[6].

In addition to the aforementioned spatially averaged quantities, instantaneous localized information is captured at three locations along the OA: Point 1 above M1, Point 2 at midpoint of OV between the telescope EA ring and fiber input unit (Figure 6), and Point 3 at the top end right above the fiber inputs. The instantaneous localized information recorded is:

- Instantaneous velocity u(t) - this provides information on local M1 wind speeds to assess mirror flushing, telescope tube and top end wind speeds to assess dome flushing and mean telescope drive torque variations since a high VF that results in high and variable velocities inside the dome is not desirable from the telescope drive control perspective.
- Instantaneous turbulent kinetic energy TKE(t) - this relates directly to the standard deviation of velocity fluctuations, and provides information on assessing wind induced image blur due to dynamic segment loading and wind jitter due to dynamic loading along the telescope tube and at the top end.

[6] Optical path differences

[7] Reduced result sets are presented for simplicity for the optical volume results show the same characteristics as the optical axis results.

4.2 Discussion of Optical Axis Results[7]

The spatial averaged volume fraction, VF(t), of outside fresh air on the optical axis (Figure 4) shows that Case 1, 4 & 5 experience better dome flushing compared to the other cases. Although all vents are open in Case 6 (as in Cases 1, 4 & 5) flushing takes longer due to the lower exterior wind speed at 2m/s. The two cases, Case 2 & 3, for which active ventilation is used, have much lower air exchange and significantly longer flushing time compared to the passively vented cases, except for the closed vent case. The worst case proves to be Case 7, for which all vents are closed, even though the outside wind speed is the highest among all cases at 10m/s.

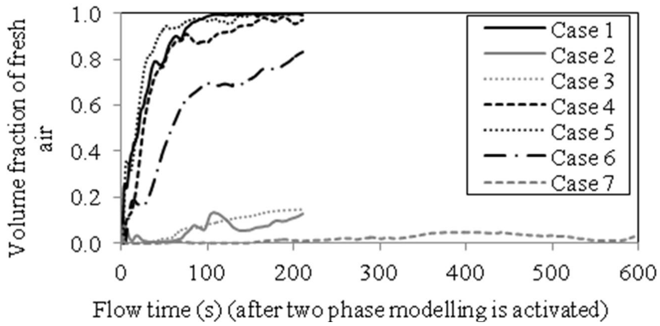

Figure 4: Spatial averaged volume fraction of fresh air on the optical axis

The spatial mean temperature, $T_{MEAN}(t)$, and RMS temperature, $T_{RMS}(t)$, on the optical axis are plotted in Figure 5. For Case 1 & 2, the enclosure air temperature is initialized at 271.3K; however for the rest of the cases 275K is used as the more practical and realistic initial temperature.

Figure 5(left) shows the mean temperature on the optical axis varies within 0.25K for Cases 3-7. Similar observation can be made for Case 1 once the mean temperature inside the enclosure stabilized by 300s of flow time. For the actively ventilated cases, the mean temperature on the optical axis does not reach to the level of the ambient temperature for Case 2 within the simulation period under the initial exhaust flow rate and initial temperature assignment.

From Figure 5(right), it can be seen that the RMS temperature varies within 0.1K for Cases 3-7, and Case 1by 300s of flow time.

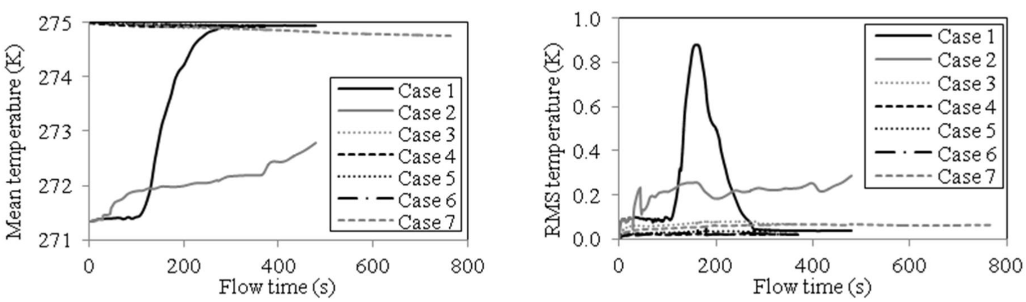

Figure 5: Spatial averaged temperature on the optical axis (left); and spatial RMS temperature on optical axis (right)

The instantaneous wind speed, u(t), and turbulent kinetic energy, TKE(t) are captured at three points along the optical axis. The results for Point 2 are plotted in Figure 6. At this location the variations in wind speed and turbulent kinetic energy are highest compared to the other two measurement points. The spikes in Figure 6 occur at the beginning of the simulations when the solution is unstable and also at the flow time when the VOF model is activated. Figure 6(left) shows highest wind speed, ~ 5m/s, at Point 2 for Case 5 compared to all other cases at <2m/s. Case 5 is the west, downwind, facing case and from the flow pattern generated we observe air flow is deflected by the telescope EA ring forming a high wind speed region inside the optical volume above Point 2 (Figure 7).

At Points 1 & 3, wind speeds are below 2 m/s for all seven cases. Again for Point 2, Case 1 & 4 show higher turbulence values, between $0.51 m^2/s^2$ to $1 m^2/s^2$, than other cases in Figure 6(right). Physically, these two cases are very similar except for the vent geometry. Therefore, we can infer that only the "common" parameters of telescope orientation and wind condition surrounding the enclosure are responsible for higher turbulence values at Point 2 for the ventilation configuration *#1-p* (Case 1) & *#2-p* (Case 4) and independent of vent geometry. For all seven cases, Points 1 and 3 show lower turbulence value of $<0.5 m^2/s^2$ than Point 2.

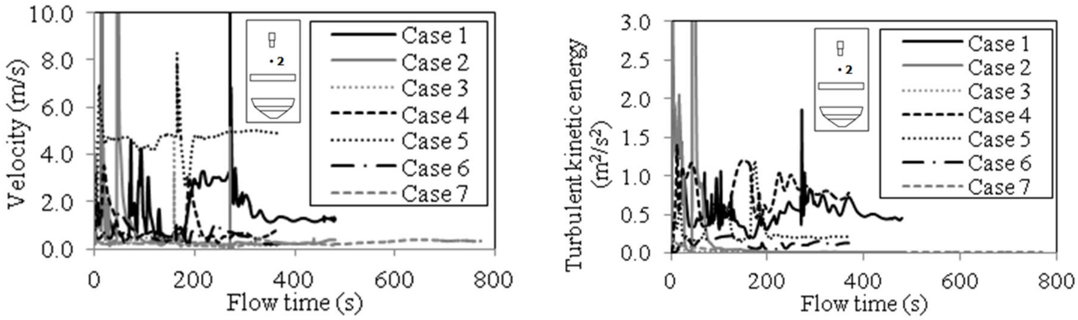

Figure 6: Instantaneous wind speed at Point 2 (left); and instantaneous turbulent kinetic energy at Point 2 (right)

Nevertheless, for all three points in all seven cases, turbulence energy is below $1 m^2/s^2$, which can be considered as favourable condition for minimal wind induced telescope dynamics.

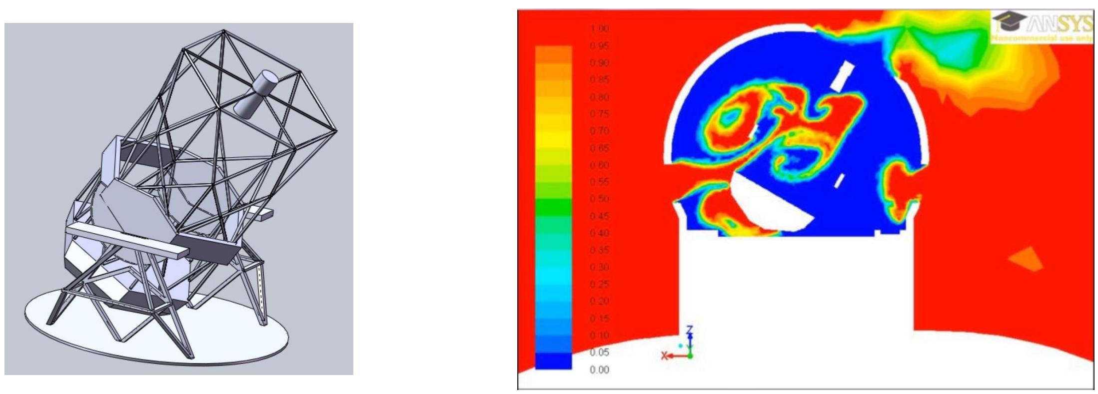
Figure 7: CDF model of telescope structure is similar to the Keck telescope with prominent hexagonal ring structure at elevation axis (left); and cross-section volume fraction profile near beginning simulation of Case 5, where bottom scale blue indicates 100% original "interior" air and top scale indicates 100% flush "exterior" air, with telescope and enclosure downwind pointing, i.e. wind flows from left to right, showing flow interaction with elevation ring resulting in a high velocity region at Point 2(right).

5. SUMMARY OF FINDINGS

The first group of three simulations, Cases 1-3, was intended to investigate which ventilation configuration minimizes dome seeing, passive or active. In Case 1, the vent openings for the ventilation configuration *#1-p* is based on our knowledge of the TMT enclosure ventilation performance thus it is not surprising the CFD result shows excellent dome flushing (Figures 8 (left) and 4), low temperature fluctuations (Figure 5) and sufficient top end wind protection. For ventilation configuration *#3-a*, the asymmetric location of the floor opening creates a circular flow pattern within the enclosure interior volume leading to insufficient fresh air exchange (Figure 8(right)). Moreover, there is bound to be higher velocities and turbulence around the top end, since the aperture is also the fresh air entrance. Depending on the relative-to-wind telescope orientation, this may or may not cause higher velocity fluctuations at the aperture opening; nevertheless, the higher wind speeds will add to telescope wind jitter. Cases 2 and 3 cannot be compared directly for temperature variations, since the Case 2 simulation has an initial temperature that is unrealistic. For Case 2, the bulk temperature inside the dome is still adjusting when the simulation ends, hence the higher temperature fluctuations. (The same should hold true for Case 1 if not for its effective passive ventilation that adjusts the bulk temperature quickly within 300s of flow time as shown in Figure 5.) However, this should not have affected the flow pattern and the fresh air volume fraction results for Case 2. Perhaps a more uniform distribution of openings around the floor would have produced better flow pattern for flushing, but we conclude the added complexity and risk associated with higher wind jitter at the top end, and ongoing operation costs for exhaust fan weigh against the active ventilation option.

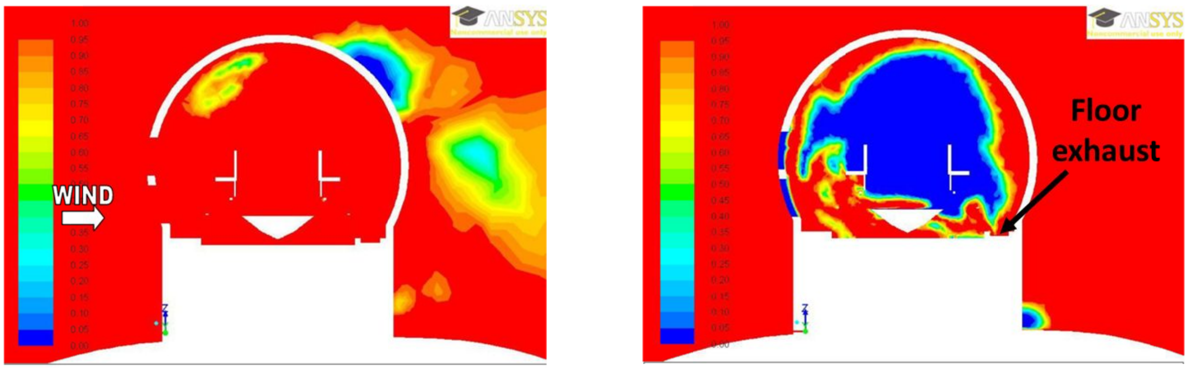

Figure 8: Cross section volume fraction profile at end of simulation where bottom scale indicates 100% original “interior” air and top scale indicates 100% flush “exterior” air. TMT type passive ventilation (Case 1) shows effective dome flushing (left) and Keck type active ventilation (Case 3) show circular interior flow with marginal exterior exchange even at 2 times the optimal exhaust flow rate (right).

To minimize construction costs and maximize simplicity, a single layer ventilation configuration *#2-p* is proposed and evaluated. Figure 9 illustrates the ventilation configuration *#2-p* as installed on the CFHT dome to demonstrate its practicality. The CFD results for Case 4 suggest that it works just as well as the two level ventilation configuration *#1-p*. Having found acceptable performance for this simplified design, three more CFD cases are conducted to assess the venting performance under different conditions: orientation change in Case 5 where the telescope and enclosure are pointing downwind; low external wind speed in Case 6; and high external wind speed in Case 7, where the vents are closed to minimize wind induced dynamics.

Figure 9: Exterior view of CFHT vents after installation (left) and interior view of CFHT vent modules during installation showing accessibility for maintenance and servicing can be achieved from the observatory floor using commercial personnel lifts without dedicated access walkway and platform attached to the enclosure structure (right).

In general, the Case 5 results suggest the ventilation configuration *#2-p* performs well under the most challenging relative-to-wind angle[8]. As stated the Calotte dome design has asymmetric venting when pointing perpendicular to wind (Case 4) but when pointing downwind (Case 5), with air coming in through the vents and out through the aperture opening, the flow is expected (and shown by the results[9]) to having higher turbulent kinetic energy. The Case 6 results suggest the ventilation configuration *#2-p* maintains reasonable flushing even at low wind speed. Finally, Case 7 verifies performance with closed vents when the external wind speed is high and provides top end protection assessment. As expected, the CDF results show the optical volume air is not exchanged as efficiently as other cases (Figure 4) but the temperature fluctuations indicate that the image quality does not suffer significantly (Figure 5&6) and the top end is also well protected. Moreover, supplemental active ventilation will not augment seeing performance in this case since at high external wind speed dome seeing is inherently worse due to the turbulent shear layer over the aperture opening, instead of the smoother flow desired at lower wind speed.

As a final conclusion, under the assumptions and (albeit limited) representative conditions simulated, the venting configuration *#2-p* for the Calotte enclosure provides the sufficient flushing to control dome seeing and top end protection for proposed telescope and enclosure concept within the context of the Feasibility Study that it is a feasible configuration that warrants further development under the MSE development plan to optimize the results.

REFERENCES

[1] A. McConnachie et al., "The Next Generation of the Canada-France-Hawaii Telescope: Science requirements and survey strategy", Proc. SPIE 8444, 844427 (2012).

[2] D. Simons et al., "Current status and future plans for Maunakea Spectrographic Explorer", Ground-based and Airborne Telescopes, ed. L. M. Stepp, R. Gilmozzi, and H. J. Hall, SPIE 9145, Montreal, Canada (2014) (this conference).

[3] A. McConnachie et al., "The Maunakea Spectrographic Explorer: science requirements and flowdown", Ground-based and Airborne Telescopes, ed. L. M. Stepp, R. Gilmozzi, and H. J. Hall, SPIE 9145, Montreal, Canada (2014) (this conference).

[4] K. Szeto et al., "Feasibility studies to upgrade the Canada-France-Hawaii Telescope site for the next generation Canada-France-Hawaii Telescope", Proc. SPIE 8444, 84440W (2012).

[5] http://www.keckobservatory.org/

[6] http://www.tmt.org/

[7] S. Roberts et al., "Systems Engineering of the Thirty Meter Telescope for the Construction Phase", Ground-based and Airborne Telescope, ed. G. Z. Angeli and P. Dierickx, SPIE 9150, Montreal, Canada (2014) (this conference).

[8] S. E. Bauman et al., "Dome venting: the path to thermal balance and superior image quality", Ground-based and Airborne Telescope, ed. A. B. Peck, C. B. Benn and R. L. Seaman, SPIE 9149, Montreal, Canada (2014) (this conference).

[9] K. Vogiatzis et al., "Local thermal seeing modeling validation through observatory measurements", Proc. SPIE 8449, 844902 (2012).

[10] M. Chun et al., "Mauna Kea ground-layer characterization campaign", Monthly Notes R. Astronomical Society 394, 1121-1130, (2009).

[11] ASCE-7, [Minimum Design Loads of Buildings and Other Structures], American Society of Civil Engineers, Reston, (2010).

[12] K. G. Thanjavur et al., "Canada-France-Hawaii Telescope image quality improvement initiative: thermal assay of the observing environment", Proc. SPIE 8444, 844464 (2012).

---

[8] Based on TMT CDF results

[9] Exaggerated by the prominent hexagonal elevation ring